Functional mapping of rbOCT1 and rbOCT2 activity in the S2 segment of rabbit proximal tubule

Santi Kaewmokul, Varanuj Chatsudthipong, Kristen K. Evans, William H. Dantzler and Stephen H. Wright

Am J Physiol Renal Physiol 285:1149-1159, 2003. First published Aug 26, 2003;
doi:10.1152/ajprenal.00112.2003

AJP - Renal Physiology publishes original manuscripts on a broad range of subjects relating to the kidney, urinary tract, and their respective cells and vasculature, as well as to the control of body fluid volume and composition. It is published 12 times a year (monthly) by the American Physiological Society, 9650 Rockville Pike, Bethesda MD 20814-3991. ISSN: 0363-6127, ESSN: 1522-1466. Visit our website at http://www.the-aps.org/.

Am J Physiol Renal Physiol 285: F1149–F1159, 2003;
10.1152/ajprenal.00112.2003.

Functional mapping of rbOCT1 and rbOCT2 activity in the S2 segment of rabbit proximal tubule

Santi Kaewmokul,[1,2] Varanuj Chatsudthipong,[1] Kristen K. Evans,[2] William H. Dantzler,[2] and Stephen H. Wright[2]

[1]*Department of Physiology, Mahidol University, Bangkok, 10700 Thailand; and* [2]*Department. of Physiology, University of Arizona, Tucson, Arizona 85724*

Submitted 21 March 2003; accepted in final form 23 August 2003

Kaewmokul, Santi, Varanuj Chatsudthipong, Kristen K. Evans, William H. Dantzler, and Stephen H. Wright. Functional mapping of rbOCT1 and rbOCT2 activity in the S2 segment of rabbit proximal tubule. *Am J Physiol Renal Physiol* 285: F1149–F1159, 2003; 10.1152/ajprenal.00112.2003.—A strategy was developed to determine the distribution of activity mediated by the organic cation (OC) transporters OCT1 and OCT2 in rabbit renal proximal tubule (RPT). Both transporters displayed similar affinities for tetraethylammonium (TEA; in CHO-K1 cells, TEA concentrations that resulted in half-maximal transport were 19.9 and 34.5 μM for OCT1 and OCT2, respectively). Similarly, some OCs showed little capacity to discriminate between the two processes (IC_{50} values for ephedrine of 13.6 and 24.2 μM for OCT1 and OCT2, respectively). However, OCT2 had a higher affinity for cimetidine and [2-(4-nitro-2,1,3-benzoxadiazol-7-yl) aminoethyl]trimethylammonium (NBD-TMA; 1.3 and 1.4 μM, respectively) than did OCT1 (97.3 and 108 μM, respectively). Conversely, OCT1 had a higher affinity for tyramine and pindolol than did OCT2 (21.2 and 2.4 vs. 361 and 50 μM, respectively). We designated these as "discriminatory inhibitors" and used them to determine the relative contribution of OCT1 and OCT2 for TEA transport in single S2 segments of rabbit RPT. Cimetidine and NBD-TMA were high-affinity inhibitors of TEA transport in S2 segments (median IC_{50} values of 12.3 and 1.4 μM, respectively); in comparison, tyramine and pindolol were low-affinity inhibitors (265 and 69.3 μM, respectively). These IC_{50} values were sufficiently close to those for OCT2 to support the conclusion that TEA transport in the S2 segment of rabbit RPT is dominated by OCT2. However, the profile of inhibition of tyramine (an OCT1-selective substrate) transport in single S2 segments indicated that, despite a comparatively low level of expression, OCT1 can play a dominant role in the uptake of selected OC substrates.

organic cation; transport; tetraethylammonium; cimetidine; kidney

ORGANIC CATIONS (and bases; collectively, OCs) constitute an extremely diverse array of compounds that include molecules of physiological, pharmacological, and toxicological importance (36). The classic OC secretory pathway of renal proximal tubules (RPT) (24) plays a central role in controlling plasma levels of many of these compounds. Studies with isolated plasma membranes (14, 15, 32, 34) and intact isolated, perfused and nonperfused renal tubules (7, 12, 27) led to the formulation and confirmation of a working model of the transport events that underlie the secretory process. In brief, OC secretion is a two-step process that involves substrate entry across the peritubular (basolateral) membrane of RPT, which appears to be dominated by electrogenic facilitated diffusion, and an exit step at the luminal (brush-border) membrane of RPT, which appears to be dominated by electroneutral mediated exchange of intracellular OC for luminal H^+. OC entry, therefore, is driven by the inside negative membrane potential of proximal tubule cells, whereas OC exit is driven by an electrochemical gradient for H^+. Although in this scheme the OC/H^+ exchanger is the active step in transepithelial OC secretion, because of its reliance on the inwardly directed electrochemical gradient for H^+, the overall process of secretion is ultimately reliant on the activity of the Na-K-ATPase and its roles in establishing the inside negative membrane potential (thereby influencing electrogenic basolateral OC entry) and the Na^+ gradient that drives activity of the Na/H exchanger (that, in turn, drives luminal OC/H^+ exchange).

Efforts to understand the cellular and molecular basis of OC secretion in RPT have been substantially advanced by the cloning of several members of a group of related transport proteins now referred to as the organic cation transporter (OCT) family of proteins (designated as 2.A.1.19 by the transport panel of the nomenclature committee of the International Union of Biochemistry and Molecular Biology) (25). Of the several OCTs that have been cloned, three of them, OCT1 (13), OCT2 (22), and OCT3 (17), have physiological characteristics consistent with those observed for the basolateral OC entry step, including an electrogenic mode of operation (see Ref. 4) and the capacity to accept a diverse range of cationic compounds as transported substrates (see Ref. 11). Immunocytochemical localization has generally shown that OCT1 and OCT2 are effectively restricted to the basolateral membrane of cells in which they are expressed (16, 21, 31). Importantly, there are marked differences in tissue distribu-

Address for reprint requests and other correspondence: S. H. Wright, Dept. of Physiology, College of Medicine, Univ. of Arizona, Tucson, AZ 85724 (E-mail: shwright@u.arizona.edu).

The costs of publication of this article were defrayed in part by the payment of page charges. The article must therefore be hereby marked "*advertisement*" in accordance with 18 U.S.C. Section 1734 solely to indicate this fact.

tion for these different OCTs. Of particular relevance to the issue addressed in the present study, in both humans and rats OCT2 mRNA expression in the kidney greatly exceeds that for OCT1 and OCT3 (21, 30). In fact, in the human kidney, immunocytochemistry failed to show any evidence for OCT1 expression in RPT, although OCT2 expression in the basolateral membrane was clearly evident (OCT3 localization has not been examined) (21). However, in the rat kidney both OCT1 and OCT2 are expressed in the basolateral membrane of RPT and are coexpressed in the S2 segment (16). It is not clear whether other common animal models of renal tubular function share characteristics of OCT distribution similar to that of the human and the rat or, instead, display a different distribution. In no species is it clear to what extent tubule localization of transporters by mRNA expression and immunocytochemistry is correlated with actual transport activity.

In the present study, we set out to develop a strategy for the "functional mapping" of OCT1 and OCT2 transport activity in a physiologically intact model of renal OC secretion. We elected to use the rabbit kidney because of its utility in studies of intact tubule function. The approach involved use of the cloned rabbit orthologs of each transporter, expressed in at least two separate expression systems, to identify "discriminatory inhibitors," i.e., compounds that preferentially interact with one or the other of the target transporters. The IC_{50} values obtained for each of these compounds against each transporter were then compared with IC_{50} values obtained in studies of basolateral OC transport activity in isolated, nonperfused single S2 segments of rabbit RPT. The inhibitory profiles obtained for both OCT1-selective and OCT2-selective inhibitors were consistent with the conclusion that OC transport in the S2 segment of rabbit RPT is dominated by OCT2. The functional mapping strategy, as outlined here, underscored both the importance of making quantitative comparisons between the results obtained with cloned transporters to those obtained in native tissue preparations and the need to exercise suitable caution when making such comparisons.

METHODS

Materials. The Chinese hamster ovarian cell line CHO-K1 and the African green monkey kidney cell line COS-7 were purchased from American Type Culture Collection (Rockville, MD). [^{3}H]tetraethylammonium (TEA) came from two sources: Amersham (Piscataway, NJ; 13.2 Ci/mmol) and the Synthesis Core of the Southwest Environmental Health Science Center of the University of Arizona (20.0 Ci/mmol). The fluorescent organic cation [2-(4-nitro-2,1,3-benzoxadiazol-7-yl) aminoethyl]trimethylammonium (NBD-TMA) was synthesized as described previously (3). All other chemicals were purchased from Sigma (St. Louis, MO) or other sources and were generally the highest purity available. Cell culture media and all other molecular biology reagents were purchased from Sigma or Life Technologies (Gaithersburg, MD). New Zealand White rabbits were purchased from Harlan (Indianapolis, IN).

Transient expression of rbOCT1 and rbOCT2 in COS-7 cells and CHO-K1 cells. COS-7 and CHO-K1 cells were grown in F-12-Ham's-Kaighn's Modification (F12K) medium supplemented with 10% fetal bovine serum, 100 U/ml of penicillin, and 100 μg/ml of streptomycin. Cells were kept in a humidified atmosphere supplied with 5% CO_2-95% air. Cells were transfected with pcDNA3.1 containing rbOCT1 or rbOCT2 (38), using electroporation (BTX model ECM 630 rev.E, Genetronics, San Diego, CA) and a method described elsewhere (2). Briefly, cells were mixed with 10 μg of desired plasmid DNA and 10 μg of salmon sperm DNA and pulsed at 260 V and 1,050 F for 20–30 ms. The cells were dispersed with a plastic transfer pipette and then plated in 12-well plates at 320,000 cells/well. The medium was changed 24 h after plating. Experiments were performed after the cells had reached confluence (normally, 48 h after plating).

Stable expression of rbOCT1 or rbOCT2 in CHO-K1 cells. CHO-K1 cells were transiently transfected with cDNAs for either rbOCT1 or rbOCT2 and after 24 h placed in culture medium supplemented with 1 mg/ml of G418 (GIBCO BRL). Surviving cells were tested for the functional expression of OC transport activity by using the fluorescent organic cation NBD-TMA, which has been shown to be a substrate for peritubular OC transport in single isolated rabbit RPT (3). Single colonies that accumulated 20 μM NBD-TMA were selected from 96-well plates. Stable clonal cell lines that expressed either rbOCT1 or rbOCT2 were grown in the selection medium and used for subsequent experiments.

Transport assays. Uptake of [^{3}H]TEA into cells expressing either rbOCT1 or rbOCT2 was measured at 25°C. After removal of the culture media, cells were washed twice with Waymouth's buffer [WB; (in mM) 135 NaCl, 13 HEPES, 28 D-glucose, 5 KCl, 1.2 $MgCl_2$, 2.5 $CaCl_2$, 0.8 $MgSO_4$, pH adjusted to 7.4 with NaOH] and then preincubated for a total of 30 min in WB (2 × 15 min). Uptake was stopped by removing the transport buffer and then rinsing the cells with three successive washes with 1 ml of ice-cold WB containing 250 μM tetrapentylammonium (TPeA). The cells were solubilized with 1% SDS in 0.2 N NaOH, neutralized with 0.4 N HCl, and transferred to scintillation vials for measurement of accumulated radioactivity (Beckman LS 3801, Beckman Instruments, Irvine, CA). Uptake rates are expressed as moles per square centimeter of surface area of the confluent monolayer.

Transport in isolated S2 segment of RPT. New Zealand White rabbits were euthanized by intravenous injection with pentobarbital sodium. The kidneys were flushed via the renal artery with an oxygenated ice-cold HEPES-sucrose solution, pH 7.4 (10 mM HEPES and 250 mM sucrose, pH adjusted with Tris base). Transverse slices of an isolated kidney were placed in a dish containing ice-chilled dissection buffer (in mM: 110 NaCl, 25 $NaHCO_3$, 5 KCl, $2Na_2HPO_4$, 1.8 $CaCl_2$, 1 $MgSO_4$, 10 sodium acetate, 8.3 D-glucose, 5 L-alanine, 4 lactate, and 0.9 glycine; pH adjusted to 7.4 with HCl or NaOH and gassed continuously with 95% O_2-5% CO_2 to maintain the pH; osmolarity of ~290 mosmol/kgH_2O). The S2 segments were manually dissected from a kidney slice at 4°C without use of enzymatic digestion. To select the S2 portion of rabbit proximal tubule, a 1- to 1.5-mm length of straight tubule was teased from a slice, starting at the cortical surface of the kidney (27). The ends of each tubule were trimmed to an average length of ~1 mm. The inhibition studies were performed in a temperature-controlled chamber at 37°C. Uptakes were measured by transferring each tubule into an oil-covered well in the chamber containing dissection buffer and radiolabeled substrate, with/without inhibitors of interest. After a 1-min incubation, uptake was stopped by trans-

ferring the tubule into microwells (60-well plate, Nunc, Naperville, IL) containing 10 μl of 1 N NaOH covered with light mineral oil. The tubules were solubilized for at least 30 min, after which the tubule extracts were transferred into small scintillation vials containing 200 μl of distilled water. The scintillation cocktail (3 ml) was added to each vial, and the radioactivity was determined using liquid scintillation spectroscopy (Beckman LS 6000 IC). At least three tubules were used to determined transport for each experimental condition tested. Transport rates were normalized to tubule length based on measurements determined from photomicrographs taken of each tubule before the experiment.

Isolation of RNA and RT-PCR. Total RNA was prepared from isolated rabbit kidney tubules following the method of Sambrook et al. (26). Immediately after euthanasia, kidneys were perfused with cold, sterile HEPES-sucrose solution (pH 7.4), removed, and placed in the same solution on ice. Slices were taken from the kidneys and kept in the same solution on ice while S2 segments were dissected. Typically, four equal groups of four to five tubule segments were transferred, along with 2 μl of buffer, to separate microfuge tubes each containing 4 μl of 2% Triton mix (89 μl sterile water, 4 μl RNase inhibitor, 5 μl 0.1 M DTT, and 2.4 μl Triton X-100). After 5 min at room temperature, the segments were frozen in liquid nitrogen and stored at −20°C until ready for RT.

Standard RT was performed on the solubilized samples, using both random primers and Oligo(dT)12–18 base pairs. Two samples had Superscript II, and the other two had water in place of Superscript II to serve as a negative control. After inactivation of the RT reaction, RNase H was added, and the samples were incubated at 37°C for 20 min to remove any remaining complementary RNA. PCR tubes were set up (50 μl total volume) using all 20 μl of RT product/PCR sample. The amount of 10× PCR buffer was adjusted to compensate for the substantial amount of first-strand buffer and to provide an appropriate concentration of $MgCl_2$. PCR tubes were also set up for rbOCT1 and rbOCT2 plasmid samples to be run as positive controls. The primers (Integrated Technologies) were as follows: for rbOCT1, a 525-bp fragment was derived from 5′-AGCTGGATGTCCGGCTA-3′ (sense) and 5′-TGGTGACCAGGATGACGA-3′ (antisense); and for rbOCT2, a 361-bp fragment was derived from 5′-GGAAGCACACCTGCATCTTG-3′ (sense) and 5′-GAGATTCCTGATGAACGTGG-3′ (antisense). All PCR samples were run simultaneously, using identical parameters, on a thermal cycler for 35 cycles. Amplified products were concentrated as needed and then separated and visualized with ethidium bromide on a 1.5% agarose gel.

RESULTS AND DISCUSSION

It was our intent to compare transport that was mediated by rbOCT1 or rbOCT2 in heterologous expression systems with the characteristics of peritubular OC transport in physiologically intact, isolated single proximal tubules. Complicating this effort was the observation that the characteristics of OCTs appeared to be influenced quantitatively by the system in which they are expressed, a fact evident in the wide range of IC_{50} values published for selected inhibitors of cloned OCTs. For example, published values for the IC_{50} of inhibition by 1-methyl-4-phenylpyridinium ion (MPP^+) of rOCT1 range from 0.8 μM in MDCK cells (33), to 13 μM in HEK 293 cells (20), to 64 μM in *Xenopus laevis* oocytes (23). Further complicating the issue was the realization that almost as large a range of values has been reported for selected substrates when expressed in the same heterologous system by different research groups. Using MPP^+ again as a representative inhibitor of rOCT1, IC_{50} values in studies using oocytes as the expression system range from 2.7 (11) to 13 (13) to 64 μM (23). Thus it is difficult to determine whether the extreme variation in quantitative characteristics of OCT-mediated transport evident in the present literature reflects differences in transporter behavior when expressed in different cell types (reflecting, for example, the influence of different regulatory pathways, or *trans*-effects arising from cell-specific differences in the concentration of cationic substrates) (e.g., 1, 5, 28) or purely technical differences (i.e., those that arise when different experimental groups perform the "same experiment" using different methodologies). Supporting the idea that differences can reflect the influence of cell type are results reported by Inui and colleagues in two parallel studies that examined the inhibitory effects of a common group of compounds on the activity of rOCT1 and rOCT2 in oocytes (23) and Madin-Darby canine kidney (MDCK) cells (33). In general, IC_{50} values measured in MDCK cells were lower than those measured in oocytes, including MPP^+ IC_{50} values for rOCT1 and rOCT2 of 0.8 and 1.8 μM in MDCK cells and 64.1 and 44.2 μM in oocytes, respectively. For cimetidine (CIM), IC_{50} values for OCT1 and OCT2 in MDCK cells were 5.7 and 9.4 μM and in oocytes were 329 and 373 μM, respectively. Lending credence to the conclusion that these marked quantitative differences in transporter behavior stemmed from the expression systems used is the fact that these measurements were made by the same research group employing, it is reasonable to assume, similar technical and analytical methods. Although it might seem reasonable a priori that the values measured in a polarized mammalian cell (i.e., MDCK cells) are more likely to reflect those observed in proximal tubule cells, there are insufficient data to support such a conclusion. Our approach was to compare results obtained with two different mammalian cell expression systems, i.e., CHO-K1 cells and COS-7 cells, with the hope of finding compounds that displayed marked selectivity for either rbOCT1 or rbOCT2. Similarities in the quantitative characteristics of substrate interactions measured in two expression systems would, we propose, lend some validity to the subsequent comparisons of these values to those measured in native tubule cells. The quantitative criteria used as the basis for such comparisons are discussed more fully below.

Time course of rbOCT1- and rbOCT2-mediated [^{3}H]TEA uptake in CHO-K1 and COS-7 cells. The first requirement was to establish the quantitative characteristics of rbOCT1 and rbOCT2 transport in the two cell lines. As shown in Fig. 1, both transporters supported time-dependent [^{3}H]TEA uptake when expressed in either cell type. In clonal lines of CHO-K1 cells in which the transporters were stably expressed, the rates of OCT1- and OCT2-mediated transport of 0.05 μM [^{3}H]TEA were approximately equivalent and comparatively rapid, with steady-state accumulation

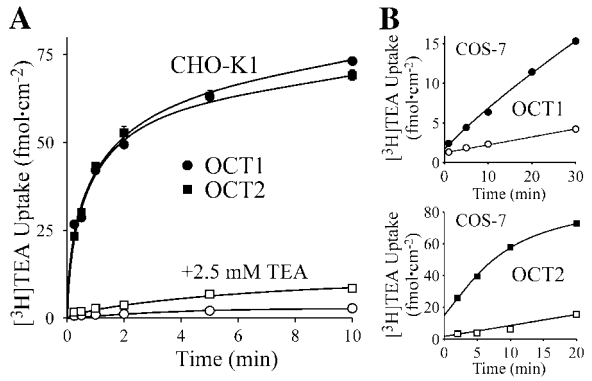

Fig. 1. Time course of [^{3}H]tetraethylammonium (TEA) uptake into Chinese hamster ovary (CHO-K1) or COS-7 cells expressing either rabbit organic cation transporter (rbOCT)1 or rbOCT2. Open symbols show the effect on this uptake of adding 2.5 mM unlabeled TEA to the media containing [^{3}H]TEA (0.05 μM). Values are means ± SE of uptakes measured in 3 separate wells in a single representative experiment.

being approached within 10 min (Fig. 1*A*). Transport in the COS-7 cells (in which the transporters were transiently transfected) was not as rapid, with transport continuing to be nearly linear for at least 20 min (Fig. 1*B*). The presence of 2.5 mM unlabeled TEA reduced the 10-min uptake of labeled substrate by 60% (OCT1 in COS-7) and by >95% (both OCT1 and OCT2 in CHO-K1 cells). Importantly, uptake of TEA into wild-type CHO-K1 and COS-7 cells was <2% of that measured in cells transfected with the cDNAs for OCT1 and OCT2 (data not shown). Thus the transport that was observed in cells transfected with OC transporter cDNAs reflected activity of those proteins. Given the profile of time-dependent transport in these cells (Fig. 1), estimates of the initial rate of TEA transport for the measurement of kinetics were typically based on 2-min uptakes in CHO-K1 cells and 5-min uptakes in COS-7 cells.

Kinetics of OCT1- and OCT2-mediated TEA transport in CHO-K1 and COS-7 cells. Figure 2*A* shows the effect of increasing concentrations of unlabeled TEA on the rate of uptake of 0.05 μM [^{3}H]TEA into a clonal line of CHO-K1 cells (*clone 7*) that stably expressed rbOCT1 or rbOCT2. The hyperbolic inhibition of [^{3}H]TEA transport was described by Michaelis-Menten kinetics of competitive interaction between labeled and unlabeled TEA (19)

$$J = \frac{J_{max}[*\,T]}{K_t + [*\,T] + [T]} + C \qquad (1)$$

where J is the rate of [^{3}H]TEA transport from a concentration of labeled substrate equal to [* T]; J_{max} is the maximum rate of mediated TEA transport; K_t is the TEA concentration that resulted in half-maximal transport (Michaelis constant); [T] is the concentration of unlabeled TEA in the transport reaction; and C is a constant that represents the component of total TEA uptake that was not saturated (over the range of substrate concentrations tested) and presumably reflects the combined influence of diffusive flux, nonspecific binding and/or incomplete rinsing of the cell layer. In three separate experiments on rbOCT1-mediated TEA transport in *clone 7* cells the K_t was 19.9 ± 1.7 μM and the J_{max} was 7.2 ± 1.4 pmol·cm^{-2}·min^{-1}. These kinetic parameters reflected the consequence of OCT1 expression in a cell population derived from a single, clonal parent cell. We sought assurance that these characteristics reflected those of OCT1 expression in a more general population of CHO-K1 cells. Consequently, we also measured the kinetics of TEA transport in three additional clonal cell lines, and in CHO-K1 cells that were transiently transfected with the cDNA for rbOCT1. The kinetic parameters of these different experiments differed principally in the maximal rate of transport, which almost certainly reflected different levels of expression (lowest, apparently, in

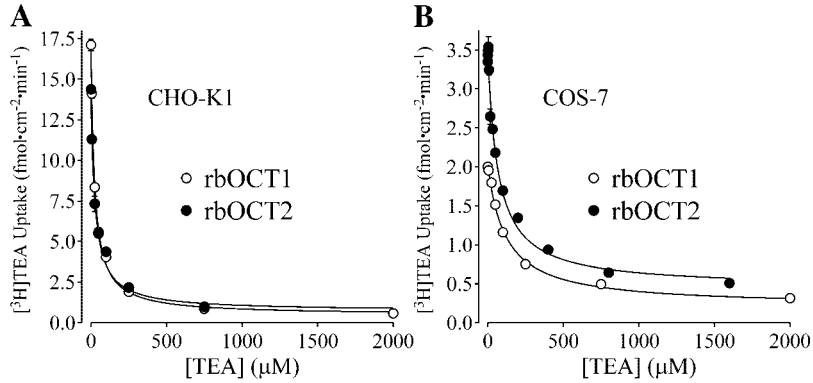

Fig. 2. Kinetics of TEA transport in CHO-K1 or COS-7 cells that stably expressed either rbOCT1 (open symbols) or rbOCT2 (solid symbols). *A*: 2-min uptakes of 0.05 μM [^{3}H]TEA were measured in CHO-K1 cells in the presence of increasing concentrations of unlabeled TEA. The kinetics of the resulting inhibition of uptake of the labeled substrate are described by the kinetics of competitive inhibition (see text). Values are means ± SE of uptakes measured in 3 wells in a single representative experiment. *B*: 5-min uptakes of 0.05 μM [^{3}H]TEA were measured in COS-7 cells in the presence of increasing concentrations of unlabeled TEA. The kinetics of the resulting inhibition of uptake of the labeled substrate are described by the kinetics of competitive inhibition (see text). Values are means ± SE of uptakes measured in 3 wells in a single representative experiment. Lines were generated using a least-squares fit of *Eq. 1* to the individual data points (SigmaPlot 3.0).

the transiently transfected cells). The Michaelis constants measured in the three additional clonal lines were 23.0, 23.1, and 19.7 μM (*n* values of 2, 1, and 1, respectively). In two experiments with transiently transfected cells, the K_t for OCT1-mediated TEA transport was 28.4 ± 2.1 μM (with a J_{max} of 0.52 ± 0.004 pmol·cm^{-2}·min^{-1}). The similarity between all these K_t values lent credence to the subsequent focus on the kinetic characteristics of *clone 7* cells.

Figure 2*A* also shows the kinetics of rbOCT2-mediated TEA uptake in a clonal line of CHO-K1 cells that stably expressed the transporter. The K_t for this transport was 34.5 ± 6.9 μM ($n = 2$) with a J_{max} of 7.9 ± 0.9 pmol·cm^{-2}·min^{-1}. The K_t for rbOCT2-mediated transport in transiently transfected CHO-K1 cells, 34.1 ± 0.4 μM (with a J_{max} of 1.3 ± 0.25 pmol·cm^{-2}·min^{-1}), was virtually identical to that measured in the stably expressing clonal cell line and, in both cases, was slightly higher than that observed for rbOCT1.

We were under no illusion that the quantitative characteristics of OCT transport expressed in CHO-K1 cells, particularly the apparent Michaelis constants of expressed transporters, would necessarily mirror those of these processes when expressed in native renal tubules. Consequently, we considered it prudent to compare the characteristics of rbOCT1 and rbOCT2 in at least one other expression system, and we chose COS-7 cells for this purpose. Figure 2*B* presents the results of representative experiments that measured the kinetics of rbOCT1 and rbOCT2 in transiently transfected COS-7 cells. For rbOCT1 the K_t was 121.0 ± 3.9 μM, with a J_{max} of 3.1 ± 0.9 pmol·cm^{-2}·min^{-1}. For rbOCT2 the K_t was 75.6 ± 8.7 μM, with a J_{max} of 3.1 ± 0.8 pmol·cm^{-2}·min^{-1}. For both transporters, the apparent affinity for TEA when expressed in COS-7 cells was less than that observed in CHO-K1 cells. The lower affinity for substrate of these transporters when expressed in COS-7 cells was a characteristic routinely observed for other putative OC substrates, as expanded on below. Comparison of these values to those reported for OCT1 and OCT2 orthologs from other species is difficult, in large part because of the large variability reported for these values, as noted earlier. However, in general, the apparent affinities of these rabbit OCTs for TEA expressed in both CHO-K1 and COS-7 cells were typically on the low side of the values reported for orthologs from other species (e.g., 6, 8, 37).

We noted previously that it is difficult to judge the extent to which quantitative differences in kinetic characteristics of cloned transporters in the literature reflect different expression systems employed or differences in technique or methodology employed to make the measurements. To this end, it is instructive to note that the K_t values for rbOCT1- and rbOCT2-mediated TEA transport in COS-7 cells reported here differ from those we reported in a previous study (38). As noted above, for OCT1, the K_t was 121.0 ± 3.9 μM; in our previous study, the K_t in transiently transfected COS-7 cells was measured as 188 ± 20 μM. For OCT2, the present value was 75.6 ± 8.7 μM, whereas it was 125 ± 22 μM in our previous study. Although these differences are comparatively small, they were measured (in some cases) on the same day, using the same cells, and the same experimental and analytic methodology; the only evident differences were those arising from a different person conducting the mechanical actions associated with the measurements. It is likely, therefore, that quantitative differences of this size and larger will occur when different research groups, employing more substantial technical differences than those in our "identical" experiments, report the results of measurements of the kinetics of substrate/inhibitor interactions with cloned transport proteins.

Discriminating inhibitors for rbOCT1 and rbOCT2. Functional mapping of OCT distribution within a defined segment of rabbit proximal tubules required identification of inhibitors for which OCT1 and OCT2 have markedly different apparent affinities. For this purpose, we examined the inhibition of TEA transport by rabbit OCT1 and OCT2 expressed in CHO-K1 and COS-7 cells. Using a similar approach, Arndt et al. (1) identified several compounds that effectively discriminated between rat OCT1 and OCT2 when expressed in *X. laevis* oocytes. For example, rOCT1 displayed a 25-fold higher apparent affinity for guanidine than did rOCT2 (IC_{50} values of 171 vs. 4,470 μM, respectively). rOCT2-selective inhibitors included procainamide and mepiperphenidol, for which OCT2 displayed 25- to 65-fold higher apparent affinities than OCT1 (IC_{50} values of 20 and 7.1 compared with 445 and 474 μM, respectively).

We determined IC_{50} values for these and several other OCs as inhibitors of TEA transport by rabbit OCT1 and OCT2 expressed in CHO-K1 cells (Table 1). Uptake of [^{3}H]TEA was measured in the presence of increasing concentrations of inhibitor, and the data were analyzed using a suitable modification of *Eq. 1* (12). Although the rabbit orthologs generally showed qualitative similarities with respect to their relative interactions with the test compounds used in the study of rat transporters by Arndt et al. (1), substantial quantitative, and sometimes, qualitative differences were noted. For example, whereas rOCT2 showed a 65-fold higher apparent affinity for mepiperphenidol than rOCT1 (1), rbOCT1 displayed a 5-fold higher affinity for mepiperphenidol than did rbOCT2 (IC_{50} values of 1.2 and 6.3 μM, respectively). Particularly striking was the very low mepiperphenidol IC_{50} for rbOCT1 (1.2 μM) (Table 1) compared with that measured for rOCT1 (474 μM) (1). rbOCT1 did show a 2-fold "preference" for procainamide over rbOCT2 (i.e., IC_{50} values of 10.8 vs. 23.0 μM) (Table 1), but this contrasted sharply with the 20-fold difference observed in the rat (1). Guanidine, on the other hand, displayed a rather similar profile of IC_{50} values for the OCT1 and OCT2 homologs in the rabbit (Table 1) and rat (1). These observations underscored the inappropriateness of assuming that substrate/inhibitor interactions measured in one species will apply in another.

In addition to guanidine, we found several compounds for which rbOCT2 had a much higher apparent affinity than rbOCT1. Figure 3 compares the inhibitor

Table 1. *Inhibition of rbOCT1- and rbOCT2-mediated [^{3}H]TEA transport by cations and weak bases*

Inhibitor	CHO-K1			COS-7		
	rbOCT1, μM	rbOCT2, μM	OCT1/OCT2	rbOCT1, μM	rbOCT2, μM	OCT1/OCT2
Isoproterenol	17.6 ± 2.2	479 ± 237	0.04			
Pindolol*	2.4 ± 0.1	50.0 ± 10.5	0.05	9.1 ± 0.5	98.5 ± 6.7	0.09
Tyramine*	21.2 ± 2.3	360.9 ± 38.0	0.06	61.5 ± 9.9	736 ± 136	0.08
Serotonin	66.7 ± 24.4	528 ± 123.2	0.13			
Mepiperphenidol	1.2 ± 0.2	6.3 ± 0.9	0.20			
Procainamide	10.8 ± 1.4	23.0 ± 1.4	0.47			
Ephedrine	13.6 ± 2.5	24.2 ± 1.4	0.56	38.5 ± 4.4	39.5 ± 1.7	0.97
Choline	740	724	1.02			
Carbachol	933	894	1.04			
BSP	94.6	60.8	1.55			
NBD-3-oxide	366	101	3.63			
Pentobarbital	77.7	19.9	3.92			
4-Phenylpyridine	81.2	16.6	4.90			
Histamine	989	200	4.94			
MPP^+	4.6	0.6	7.68			
NMN	994	101	9.79			
Guanidine	4,902 ± 1,581	269	18.2			
Imidazole	536	20.5	26.2			
NBD-TMA*	108 ± 7.2	1.4 ± 0.2	75.1	274 ± 35.6	3.1 ± 0.1	88.4
Cimetidine*	97.3 ± 3.3	1.3 ± 0.2	78.0	164 ± 11.9	2.9 ± 0.3	56.6

Values are means ± SE of IC_{50} values determined in 2 or 3 separate experiments. rbOCT, rabbit organic cation transporter; BSP, sulfobromophthalein; NBD, [2-(4-nitro-2,1,3-benzoxadiol-7-yl)aminoethyl]; MPP^+, 1-methyl-4-phenylpyridinium ion; NMN, *N*-methylnicotinamide; TMA, trimethylammonium; TEA, tetraethylammonium. The IC_{50} for each compound was determined by assessing its inhibition of TEA transport into either Chinese hamster ovary (CHO-K1) cells or COS-7 cells expressing the rabbit orthologs of rbOCT1 or rbOCT2. The inhibitors are listed in ascending order of the ratio of IC_{50} values, OCT1/OCT2, as determined in CHO-K1 cells. *Discriminatory inhibitors selected for studies with intact tubules.

profiles for two of these, i.e., CIM and NBD-TMA. In three separate experiments, the IC_{50} values for CIM inhibition of TEA transport by rbOCT1 and rbOCT2 were 97.3 ± 3.3 and 1.3 ± 0.2 μM. In other words, when expressed in CHO-K1 cells the apparent affinity of rbOCT2 for CIM was ~75 times higher than that of rbOCT1. This result is qualitatively similar to that we reported previously in a study that compared CIM interaction with rbOCT1 and rbOCT2 expressed in COS-7 cells (38). In that study the IC_{50} values for CIM inhibition of TEA transport by OCT1 and OCT2 were 916 and 5.7 μM, respectively, representing a 160-fold difference in apparent affinity of the two homologues

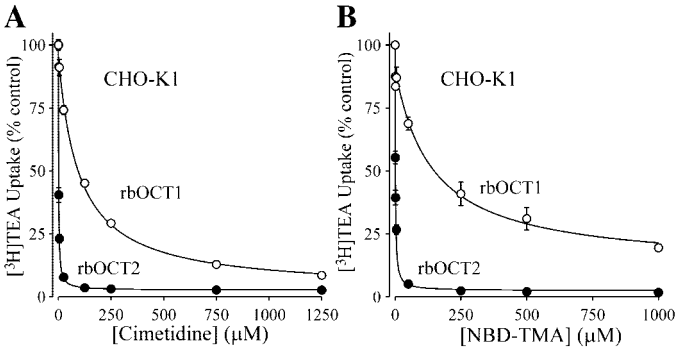

Fig. 3. Kinetics of inhibition by cimetidine (*A*) or [2-(4-nitro-2,1,3-benzoxadiazol-7-yl) aminoethyl]trimethylammonium (NBD-TMA; *B*) of TEA transport into CHO-K1 cells mediated by either rbOCT1 (open symbols) or rbOCT2 (solid symbols). Two-minute uptakes of 0.05 μM [^{3}H]TEA were measured in the presence of increasing concentrations of inhibitor. Values are means ± SE of uptakes measured in 3 wells in a single representative experiment.

for CIM. The second compound that displayed a marked preference for OCT2 was the fluorescent cation NBD-TMA (Fig. 3*B*). In three separate experiments, the IC_{50}s for NBD-TMA's inhibition of TEA transport by rbOCT1 and rbOCT2 were 108.4 ± 7.2 and 1.4 ± 0.2 μM, respectively; i.e., the apparent affinity of rbOCT2 for NBD-TMA was ~75 times higher than that of rbOCT1 (Table 1).

rbOCT1 displayed a markedly higher apparent affinity for several test agents than did rbOCT2 (Table 1). Figure 4 compares the inhibitor profiles for two of these, pindolol and tyramine. In three separate experiments, the IC_{50} values for pindolol's inhibition of TEA transport by rbOCT1 and rbOCT2 were 2.4 ± 0.1 and 50.0 ± 10.5 μM, respectively. For tyramine, the IC_{50} values for rbOCT1 and rbOCT2 were 21.2 ± 2.3 and 360.9 ± 21.9 μM, respectively. Thus for these two substrates, the apparent affinity of rbOCT1 was ~17–20-times higher than that of rbOCT2 (Table 1). Figure 5 compares the ratios of rbOCT1 and rbOCT2 IC_{50} values for six of the test compounds. Although the transporters do show preferential interaction with selected compounds, they interact with other molecules, e.g., TEA and ephedrine, with virtually identical kinetics (Fig. 5 and Table 1). The existence of such "nondiscriminating" substrates is of particular value with respect to identifying fractional contribution of different transport proteins to total substrate uptake by intact tubules, as discussed below.

As noted earlier, we routinely compared the characteristics of OCT1 and OCT2 observed in CHO-K1 cells with those observed in COS-7 cells. Table 1 lists the

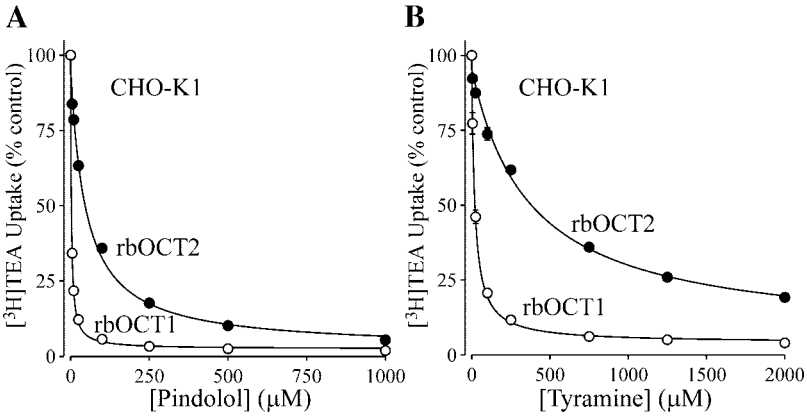

Fig. 4. Kinetics of inhibition by pindolol (*A*) or tyramine (*B*) of TEA transport into CHO-K1 cells mediated by either rbOCT1 (open symbols) or rbOCT2 (solid symbols). Two-minute uptakes of 0.05 μM [^{3}H]TEA were measured in the presence of increasing concentrations of inhibitor. Values are means ± SE of uptakes measured in 3 wells in a single representative experiment.

IC_{50} values for the test agents examined in this study, as inhibitors of TEA transport by rbOCT1 and rbOCT2 when expressed (stably) in CHO-K1 cells or (transiently) in COS-7 cells. Importantly, the profile of inhibition observed in CHO-K1 was also observed, at least qualitatively, in COS-7 cells. In other words, compounds that were potent inhibitors of the transporters in CHO-K1 cells were also comparatively potent inhibitors of these processes when expressed in COS-7 cells. This is graphically emphasized in Fig. 6, which plots for each transporter the measured IC_{50} or K_t values for six different compounds as determined in the present study for both CHO-K1 and COS-7. Both transporters consistently displayed higher apparent affinities for substrates or inhibitors in CHO-K1 cells. The lower affinity of the transporters in COS-7 cells was quite consistent, with IC_{50} values being 2.6 ± 0.25 times higher in COS-7 cells than in CHO-K1 cells over the full range of affinities observed (Fig. 6).

Effect of OCT-homologue-specific inhibitors on TEA transport in single rabbit S2 proximal tubule segments. There are clear species differences in the distribution and expression level of different OCTs in the RPT. Whereas OCT expression in the human RPT appears to be dominated by OCT2 (21), OCT1 and OCT2 are both expressed in rat RPT (16). Indeed, OCT1 and OCT2 appear to be coexpressed in the S2 segment of the rat RPT, with the S1 segment being dominated by OCT1 expression and the S3 segment being dominated by OCT2 expression. The fact that we cloned both OCT1 and OCT2 from mRNA isolated from rabbit renal cortex suggests that both homologues are expressed in the rabbit RPT. However, the relative expression level and functional distribution of these processes in the rabbit are not clear.

In developing a map of functional OCT expression in rabbit RPT, we elected to first focus on the S2 segment. In addition to being less technically challenging (than working with isolated S1 and S3 segments), the S2 segment, based on the results obtained with rat kidney noted above (16), was considered the most likely site for coexpression of OCT1 and OCT2. Therefore, to establish the relative contribution of OCT1 and OCT2 to basolateral OC transport in S2 segments of rabbit RPT, we determined the effect of several discriminating inhibitors of OCT transport on TEA uptake into isolated single S2 proximal tubule segments (Table 2). Recall that, as a nondiscriminating substrate, TEA displayed comparatively equal affinity for rbOCT1 and rbOCT2 (Fig. 5). Figure 7 shows the inhibition profiles produced by NBD-TMA (selective inhibitor of rbOCT2)

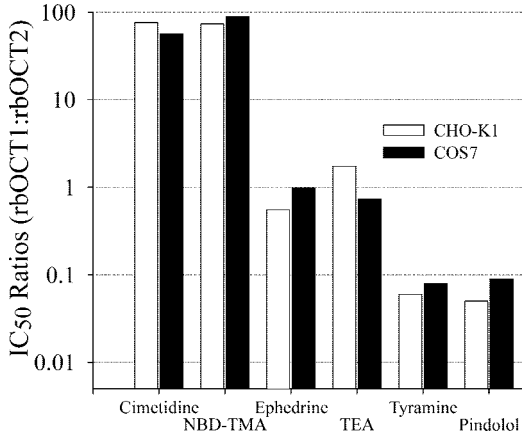

Fig. 5. Ratio of the IC_{50} values for inhibition of rbOCT1 to the IC_{50} values for inhibition of rbOCT2. Determinations in CHO-K1 cells are shown as open bars and determinations in COS-7 cells as filled bars.

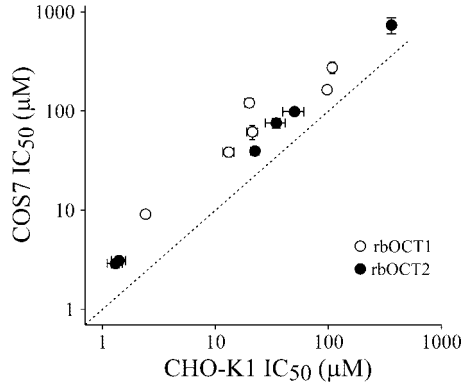

Fig. 6. Comparison of IC_{50} values measured for inhibition of rbOCT1 (open symbols) or rbOCT2 (filled symbols) expressed in either CHO-K1 cells or COS-7 cells. The dotted line depicts equal values for the 2 cell types. Values are means ± SE of IC_{50} values measured in several separate experiments (typically, 3 for CHO-K1 cells and 2 for COS-7 cells).

Table 2. *Inhibition of [^{3}H]TEA transport into isolated single S2 segments of rabbit proximal tubule produced by discriminatory inhibitors of rbOCT1 or rbOCT2*

Inhibitor	IC_{50}, μM
Cimetidine (5)	19.5 ± 8.4 Median = 12.3
NBD-TMA (4)	8.6 ± 7.6 Median = 1.4
Tyramine (3)	386 ± 122 Median = 265
Pindolol (5)	73.0 ± 14.3 Median = 69.3

Values are means ± SE with no. of experiments in parentheses. Data for cimetidine are from Ref. 38.

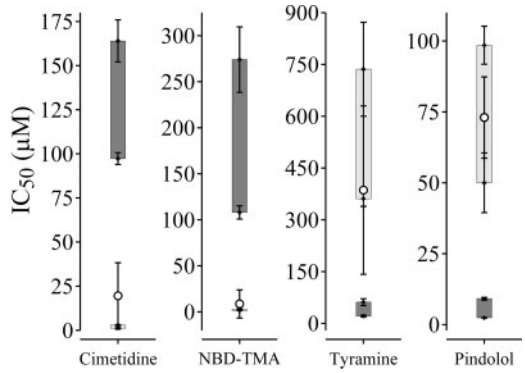

Fig. 8. Comparison of IC_{50} values determined for several organic cations that serve as discriminatory inhibitors of TEA transport mediated by either rbOCT1 or rbOCT2. The dark gray bars depict the range of IC_{50} values determined for inhibition of rbOCT1 as expressed in either CHO-K1 cells or COS-7 cells, and the light gray bars depict the range of IC_{50} values determined for inhibition of rbOCT2 as expressed in either CHO-K1 cells or COS-7 cells. In each case, the higher end of the range (shown as a solid point ± SE) indicates the value determined in COS-7 cells. Each open circle shows the mean ±SD IC_{50} value for inhibition of mediated TEA uptake into isolated, single nonperfused S2 segments of rabbit RPT. For all 4 discriminatory agents, the profile of inhibition of TEA uptake into RPT coincided with the selectivity characteristics of rabbit OCT2.

and by pindolol and tyramine (selective inhibitors of rbOCT1). Figure 8 compares the intact tubule IC_{50} values for these discriminating inhibitors (Table 2) with those obtained for the cloned transporters in heterologous expression systems (Table. 1).

As noted earlier, there is no a priori basis for assuming that the kinetic characteristics observed in CHO-K1 cells will be more representative of those expressed in native proximal tubules than the kinetic characteristics observed in COS-7 cells (or any other heterologous expression system). The K_t for basolateral TEA uptake measured in isolated single rabbit RPT is on the order of 110 μM (12). Although this value is closer to those measured here in COS-7 cells (121 and 75.6 μM for rbOCT1 and rbOCT2, respectively) than in CHO-K1 cells (19.9 and 34.5 μM, respectively), we considered it prudent to compare the IC_{50} values measured in intact tubules to those measured in both heterologous expression systems.

Figure 8 includes a graphical representation of the range of IC_{50} values for both homologues determined in CHO-K1 and COS-7 cells. The light gray-shaded bars indicate the range of OCT2 IC_{50} values obtained for the two cell types, and the dark gray bars indicate the range of OCT1 IC_{50} values. The open circles represent the mean ± SD IC_{50} for inhibition of basolateral TEA uptake in S2 segments of rabbit RPTs by each discriminating inhibitor, including data obtained in a previous study that compared the IC_{50} value for CIM inhibition of TEA transport in intact S2 segments of rabbit RPTs with that measured for rbOCT1- or rbOCT2-mediated transport of TEA into transiently transfected COS-7 cells (38). The comparatively low median IC_{50} value for CIM inhibition of tubular transport of 12 μM measured in that study was sufficiently similar to that measured for OCT2-mediated transport (6 μM), and sufficiently different from that measured for OCT1-mediated transport (~700–900 μM), to support the conclusion that basolateral TEA transport in the S2 segment of rabbit proximal tubules is probably dominated by OCT2 activity (38). Here we extend those observations to include the inhibitory profiles of another OCT2-selective inhibitor (NBD-TMA) and, importantly, two OCT1-selective inhibitors (tyramine and pindolol). If our previous conclusion was correct, low concentrations of NBD-TMA should block tubular TEA transport, whereas comparatively high concentrations of tyramine and pindolol will be required to block TEA uptake. In fact, as shown in Figure 8, both CIM and NBD-TMA blocked tubular TEA uptake to a degree consistent with uptake activity being dominated by OCT2. The inhibitor profiles produced by tyramine and

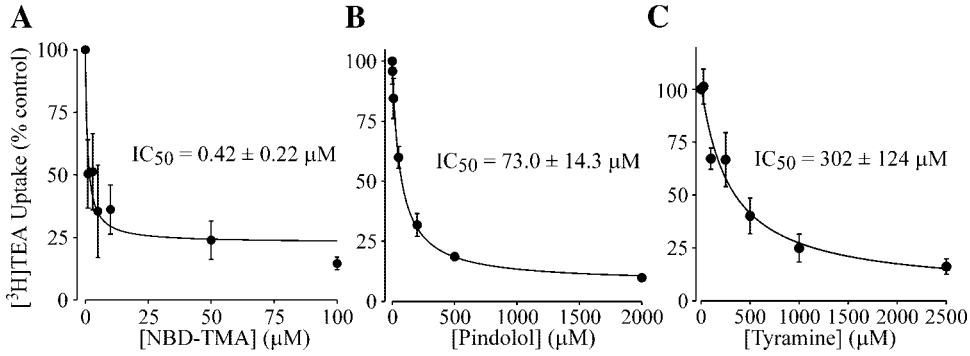

Fig. 7. Kinetics of inhibition by NBD-TMA (*A*), pindolol (*B*), or tyramine (*C*) of [^{3}H]TEA uptake into isolated, single nonperfused S2 segments of rabbit renal proximal tubule (RPT). Values are means ± SE of triplicate 1-min uptakes of labeled TEA (0.5–2.0 μM) measured in separate experiments with 3–5 different rabbits.

pindolol, each comparatively poor inhibitors of tubular TEA transport, were also consistent with basolateral OC transport's being dominated by OCT2, rather than OCT1.

TEA is not a discriminating substrate, i.e., it is handled with comparatively equal facility by rbOCT1 and rbOCT2 (Fig. 2). Consequently, it was of interest to determine whether expression of OCT1, albeit at low levels, in the S2 segment could be rendered evident by examining transport of the OCT1 distinguishing substrate, tyramine. We first confirmed that, as suggested by tyramine's inhibition of TEA transport, OCT1 displays a substantially higher apparent affinity for tyramine than OCT2: K_t of 23.1 ± 10.5 (n = 4) and 590 ± 175 μM (n = 3), respectively (J_{max} of 12.1 ± 4.8 and 92 ± 36.4 pmol·cm^{-2}·min^{-1}). If OCT1 is expressed at very low levels in the S2 segment, then it is likely that half-saturation of basolateral tyramine uptake would reflect the influence of a low-affinity interaction with OCT2, rather than a high-affinity interaction with OCT1. In fact, the half-saturation constant for basolateral tyramine uptake was 122 ± 49.6 μM (n = 3) (Fig. 9*A*), intermediate in value to the apparent K_t for uptake mediated by rabbit OCT1 and OCT2 (in CHO cells). Although this intermediate value could reflect the influence of expression in the native tubule, compared with CHO cells, it could also be explained by the influence of coexpression of OCT1 and OCT2 in the S2 segment, with the former at much lower levels than the latter. Thus OCT2 activity would dominate uptake of a nondistinguishing substrate, such as TEA, whereas OCT1 activity would become evident during uptake of an OCT1-selective substrate, such as tyramine. Although, in principle, computational methods can be used to establish the parallel activity of high- and low-affinity pathways, it was impractical to devise experiments with single tubules that cover with high precision a sufficiently broad range of substrate concentrations. Nevertheless, the profile of CIM's inhibition of tyramine transport did provide a profile that was qualitatively consistent with the presence of a modest level of expression of OCT1 in parallel with a comparatively large expression of OCT2. Figure 9*B* shows the profile of CIM's inhibition of tyramine uptake into single S2 segments. The solid line was derived using the mean IC_{50} as determined assuming that mediated (i.e., saturable) tyramine uptake involved a single process. Recalling that CIM blocks OCT2 with an IC_{50} of 1–10 μM, the high IC_{50} value for inhibition of tyramine uptake is strong evidence that OCT1 is expressed in the S2 segment. However, what of the influence of OCT2 to tyramine transport? Its low affinity for tyramine suggests it would play a modest role in tracer tyramine transport, but the fraction of total tyramine transport that is mediated by OCT2, albeit modest, should be blocked efficiently by CIM. Inspection of the CIM inhibition profile reveals that the "one-pathway" model provided a comparatively poor fit to the data at both high and low concentrations of CIM (see Fig. 9*B*, *inset*). The dashed line in the *inset* was calculated using a model that included two mediated avenues for tyramine transport, one of high affinity (apparent IC_{50} of ~10 μM) for CIM and responsible for ~25% of tracer tyramine uptake; and one of low affinity (IC_{50} of ~1 mM) responsible for the other 75% of mediated tracer tyramine uptake. We suggest that the first of these represents the activity of OCT2, whereas the second represents the activity of OCT1.

The profile of transport function in the S2 segment of rabbit RPT is consistent with quantitatively significant roles for both OCT1 and OCT2. The comparatively high level of OCT2 expression makes it likely to dominate tubular uptake of substrates that can share either process (as well as those that show a marked selectivity for OCT2, of course). However, OCT1 appears to be expressed at sufficient levels to make it the predominant pathway for entry of substrates that are transported by both processes but show a marked degree of selectivity for OCT1.

Distribution of OCT1 and OCT2 mRNA in S2 segments of rabbit RPT. In a previous study we compared levels of expression of mRNA for OCT1 and OCT2 in single S2 segments of RPT using the method of RT-PCR (38). In that study, whereas an OCT2-specific product was amplified in all the individual segments tested, we failed to amplify an OCT1-specific product. In the light of the present observations that argue for the expression, albeit at functionally low levels, of

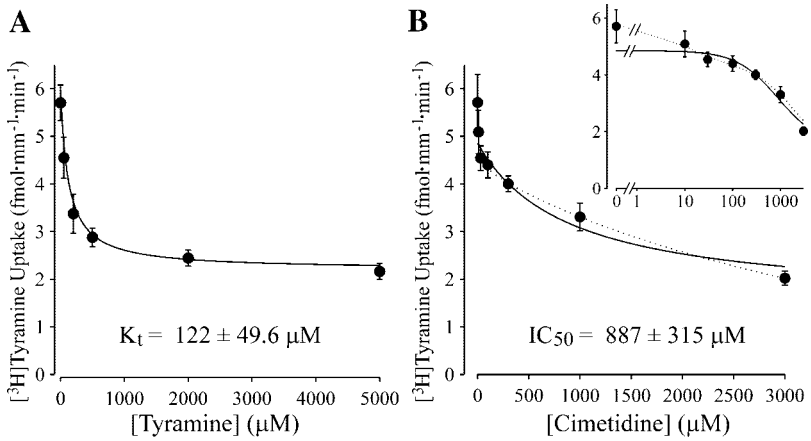

Fig. 9. *A*: kinetics of [^{3}H]tyramine uptake into isolated, single nonperfused S2 segments of rabbit RPT. Values are means ± SE of triplicate 1-min uptakes of labeled tyramine (0.4 μM) measured in separate experiments with 3 different rabbits. *B*: kinetics of cimetidine's inhibition of [^{3}H]tyramine uptake into isolated, single nonperfused S2 segments of rabbit RPT. Values are means ± SE of triplicate 1-min uptakes of labeled tyramine (0.4 μM) measured in separate experiments with 5 different rabbits. The solid line is calculated assuming the influence of a single mediated process, whereas the dotted line assumes the presence of 2 mediated processes (see text). *Inset*: semi-log transform of the data on cimetidine inhibition of tyramine uptake into single S2 segments (units the same as those in *B*).

OCT1 as well as OCT2 in the rabbit S2 segment, we reexamined the expression of transporter mRNA in isolated tubule segments. Whereas OCT2 mRNA was noted in eight of the nine rabbits tested for OCT2, OCT1 mRNA was found in only two of the eight rabbits tested for OCT1 (the identity of the amplified product was confirmed by sequence analysis). These data are consistent with the contention that OCT2 is expressed at consistently higher levels in the S2 segment of rabbit RPT than is OCT1.

The typically low expression level of OCT1 in the S2 segment of the rabbit RPT should not be interpreted as evidence for similarly low levels of expression in other segments of the RPT or, possibly, other regions of the nephron. There is also evidence of mediated TEA transport in isolated rat distal, as well as proximal, renal tubules (9), and the expression of OCT2 in rabbit distal tubules cannot be excluded. Gourbelov et al. (10) suggested that the low level of OCT1 expression in the human kidney, compared with OCT2 expression, was consistent with a general housekeeping role for this process.

The present data do not allow a conclusion to be drawn about the possible contribution of OCT3 to TEA uptake in the S2 segment. OCT3 is expressed in both human and rat kidney (21, 30), and it does accept TEA as a substrate (17, 35). However, OCT3 mRNA is expressed at much lower levels than OCT2 mRNA in both the human (21) and the rat (30). In addition, the affinity of rat and mouse OCT3 for TEA is much lower than that of either OCT1 or OCT2 (17, 35). Consequently, we consider it unlikely that OCT3 plays a major role in mediating transport of TEA (or other OCs) in the rabbit RPT.

In conclusion, the present study used the profile of transport inhibition in isolated rabbit RPT to show that basolateral TEA uptake in isolated single S2 segments is dominated by the activity of OCT2 and that functional expression of OCT1 is typically very low. Nevertheless, sufficient levels of OCT1 activity were noted to make it likely that it can play a major role in tubular transport of those substrates that show a marked selectivity for OCT1 over OCT2. Differential expression of these two transporters (or expression of their polymorphic variants) (18, 29) could result in marked changes in patterns of tubular secretion of cationic substrates. This study was also used to establish a functional mapping strategy that can be used to examine the physiological distribution of homologous transport proteins within defined segments of the RPT. The method depends on the identification of discriminating substrates/inhibitors that clearly distinguish between the activities of the different homologous processes under study. In addition, the demonstration of systematic differences in the kinetic profile of cloned transport proteins when expressed in different heterologous systems serves as a cautionary warning. The present results argue that functional mapping of transport activity in renal tubules is most prudently based on comparisons of activity of cloned transporters that are expressed in several different expression systems with the activity of those processes expressed in the native tissue of the same species. To that end, the rabbit offers an excellent experimental system for such studies because the availability of cloned transport proteins is readily matched with the comparative ease of study of single defined RPT segments.

DISCLOSURES

The authors appreciate the support of the Royal Golden Jubilee program (Thailand Research Fund Grant PHD/00166/2541). In addition, this work was supported in part by National Institutes of Health Grants DK-58251, ES-04940, ES-06694, and HL-07249.

REFERENCES

1. **Arndt P, Volk C, Gorboulev V, Budiman T, Popp C, Ulzheimer-Teuber I, Akhoundova A, Koppatz S, Bamberg E, Nagel G, and Koepsell H.** Interaction of cations, anions, and weak base quinine with rat renal cation transporter rOCT2 compared with rOCT1. *Am J Physiol Renal Physiol* 281: F454–F468, 2001.
2. **Barendt WM and Wright SH.** The human organic cation transporter (hOCT2) recognizes the degree of substrate ionization. *J Biol Chem* 277: 22491–22496, 2002.
3. **Bednarczyk D, Mash EA, Aavula BR, and Wright SH.** NBD-TMA: a novel fluorescent substrate of the peritubular organic cation transporter of renal proximal tubules. *Pflügers Arch* 440: 184–192, 2000.
4. **Busch AE, Quester S, Ulzheimer JC, Waldegger S, Gorboulev V, Arndt P, Lang F, and Koepsell H.** Electrogenic properties and substrate specificity of the polyspecific rat cation transporter rOCT1. *J Biol Chem* 271: 32599–32604, 1996.
5. **Cetinkaya I, Ciarimboli G, Yalcinkaya G, Mehrens T, Velic A, Hirsch JR, Gorboulev V, Koepsell H, and Schlatter E.** Regulation of human organic cation transporter hOCT2 by PKA, PI3K, and calmodulin-dependent kinases. *Am J Physiol Renal Physiol* 284: F293–F302, 2003.
6. **Chen R and Nelson JA.** Role of organic cation transporters in the renal secretion of nucleosides. *Biochem Pharmacol* 60: 215–219, 2000.
7. **Dantzler WH, Brokl O, and Wright SH.** Brush-border TEA transport in intact proximal tubules and isolated membrane vesicles. *Am J Physiol Renal Fluid Electrolyte Physiol* 256: F290–F297, 1989.
8. **Dresser MJ, Gray AT, and Giacomini KM.** Kinetic and selectivity differences between rodent, rabbit, and human organic cation transporters (OCT1). *J Pharmacol Exp Ther* 292: 1146–1152, 2000.
9. **Goralski KB and Sitar DS.** Tetraethylammonium and amantadine identify distinct organic cation transporters in rat renal cortical proximal and distal tubules. *J Pharmacol Exp Ther* 290: 295–302, 1999.
10. **Gorboulev V, Ulzheimer JC, Akhoundova A, Ulzheimer-Teuber I, Karbach U, Quester S, Baumann C, Lang F, Busch AE, and Koepsell H.** Cloning and characterization of two human polyspecific organic cation transporters. *DNA Cell Biol* 16: 871–881, 1997.
11. **Gorboulev V, Volk C, Arndt P, Akhoundova A, and Koepsell H.** Selectivity of the polyspecific cation transporter rOCT1 is changed by mutation of aspartate 475 to glutamate. *Mol Pharmacol* 56: 1254–1261, 1999.
12. **Groves CE, Evans K, Dantzler WH, and Wright SH.** Peritubular organic cation transport in isolated rabbit proximal tubules. *Am J Physiol Renal Fluid Electrolyte Physiol* 266: F450–F458, 1994.
13. **Gründemann D, Gorboulev V, Gambaryan S, Veyhl M, and Koepsell H.** Drug excretion mediated by a new prototype of polyspecific transporter. *Nature* 372: 549–552, 1994.
14. **Holohan PD and Ross CR.** Mechanisms of organic cation transport in kidney plasma membrane vesicles. 1. Countertransport studies. *J Pharmacol Exp Ther* 215: 191–197, 1980.

15. **Holohan PD and Ross CR.** Mechanisms of organic cation transport in kidney plasma membrane vesicles. 2. ΔpH studies. *J Pharmacol Exp Ther* 216: 294–298, 1981.
16. **Karbach U, Kricke J, Meyer-Wentrup F, Gorboulev V, Volk C, Loffing-Cueni D, Kaissling B, Bachmann S, and Koepsell H.** Localization of organic cation transporters OCT1 and OCT2 in rat kidney. *Am J Physiol Renal Physiol* 279: F679–F687, 2000.
17. **Kekuda R, Prasad PD, Wu X, Wang H, Fei YJ, Leibach FH, and Ganapathy V.** Cloning and functional characterization of a potential-sensitive, polyspecific organic cation transporter (OCT3) most abundantly expressed in placenta. *J Biol Chem* 273: 15971–15979, 1998.
18. **Leabman MK, Huang CC, Kawamoto M, Johns SJ, Stryke D, Ferrin TE, DeYoung J, Taylor T, Clark AG, Herskowitz I, and Giacomini KM.** Polymorphisms in a human kidney xenobiotic transporter, OCT2, exhibit altered function. *Pharmacogenetics* 12: 395–405, 2002.
19. **Malo C and Berteloot A.** Analysis of kinetic data in transport studies: new insights from kinetic studies of Na^+-D-glucose cotransport in human intestinal brush-border membrane vesicles using a fast sampling, rapid filtration apparatus. *J Membr Biol* 122: 127–141, 1991.
20. **Martel F, Vetter T, Russ H, Gründemann D, Azevedo I, Koepsell H, and Schömig E.** Transport of small organic cations in the rat liver. The role of the organic cation transporter OCT1. *Naunyn-Schm Arch Pharmacol* 354: 320–326, 1996.
21. **Motohashi H, Sakurai Y, Saito H, Masuda S, Urakami Y, Goto M, Fukatsu A, Ogawa O, and Inui KI.** Gene expression levels and immunolocalization of organic anion transporters in the human kidney. *J Am Soc Nephrol* 13: 866–874, 2002.
22. **Okuda M, Saito H, Urakami Y, Takano M, and Inui KI.** cDNA cloning and functional expression of a novel rat kidney organic cation transporter, OCT2. *Biochem Biophys Res Commun* 224: 500–507, 1996.
23. **Okuda M, Urakami Y, Saito H, and Inui K.** Molecular mechanisms of organic cation transport in OCT2-expressing *Xenopus* oocytes. *Biochim Biophys Acta* 1417: 224–231, 1999.
24. **Pritchard JB and Miller DS.** Mechanisms mediating renal secretion of organic anions and cations. *Physiol Rev* 73: 765–796, 1993.
25. **Saier MH Jr.** A functional-phylogenetic classification system for transmembrane solute transporters. *Microbiol Mol Biol Rev* 64: 354–411, 2000.
26. **Sambrook J, Fritsch EF, and Maniatis T.** *Molecular Cloning: A Laboratory Manual*. Cold Spring Harbor, NY: Cold Spring Harbor, 1989.
27. **Schäli C, Schild L, Overney J, and Roch-Ramel F.** Secretion of tetraethylammonium by proximal tubules of rabbit kidneys. *Am J Physiol Renal Fluid Electrolyte Physiol* 245: F238–F246, 1983.
28. **Schlatter E, Monnich V, Cetinkaya I, Mehrens T, Ciarimboli G, Hirsch JR, Popp C, and Koepsell H.** The organic cation transporters rOCT1 and hOCT2 are inhibited by cGMP. *J Membr Biol* 189: 237–244, 2002.
29. **Shu Y, Leabman MK, Feng B, Mangravite LM, Huang CC, Stryke D, Kawamoto M, Johns SJ, DeYoung J, Carlson E, Ferrin TE, Herskowitz I, and Giacomini KM.** Evolutionary conservation predicts function of variants of the human organic cation transporter, OCT1. *Proc Natl Acad Sci USA* 100: 5902–5907, 2003.
30. **Slitt AL, Cherrington NJ, Hartley DP, Leazer TM, and Klaassen CD.** Tissue distribution and renal developmental changes in rat organic cation transporter mRNA levels. *Drug Metab Dispos* 30: 212–219, 2002.
31. **Sweet DH and Pritchard JB.** rOCT2 is a basolateral potential-driven carrier, not an organic cation/proton exchanger. *Am J Physiol Renal Physiol* 277: F890–F898, 1999.
32. **Takano M, Inui KI, Okano T, Saito H, and Hori R.** Carrier-mediated transport systems of tetraethylammonium in rat renal brush-border and basolateral membrane vesicles. *Biochim Biophys Acta* 773: 113–124, 1984.
33. **Urakami Y, Okuda M, Masuda S, Saito H, and Inui KI.** Functional characteristics and membrane localization of rat multispecific organic cation transporters, OCT1 and OCT2, mediating tubular secretion of cationic drugs. *J Pharmacol Exp Ther* 287: 800–805, 1998.
34. **Wright SH and Wunz TM.** Transport of tetraethylammonium by rabbit renal brush-border and basolateral membrane vesicles. *Am J Physiol Renal Fluid Electrolyte Physiol* 253: F1040–F1050, 1987.
35. **Wu X, Huang W, Ganapathy ME, Wang H, Kekuda R, Conway SJ, Leibach FH, and Ganapathy V.** Structure, function, and regional distribution of the organic cation transporter OCT3 in the kidney. *Am J Physiol Renal Physiol* 279: F449–F458, 2000.
36. **Zhang L, Brett CM, and Giacomini KM.** Role of organic cation transporters in drug absorption and elimination. *Annu Rev Pharmacol Toxicol* 38: 431–460, 1998.
37. **Zhang L, Schaner ME, and Giacomini KM.** Functional characterization of an organic cation transporter (hOCT1) in a transiently transfected human cell line (HeLa). *J Pharmacol Exp Ther* 286: 354–361, 1998.
38. **Zhang X, Evans KK, and Wright SH.** Molecular cloning of rabbit organic cation transporter rbOCT2 and functional comparisons with rbOCT1. *Am J Physiol Renal Physiol* 283: F124–F133, 2002.